Probability of Error for Diversity Combining in DS CDMA Systems with Synchronization Errors †

M. Oğuz Sunay and Peter J. McLane ‡

Abstract

An efficient series that is used to calculate the probability of error for a BPSK modulated DS CDMA system with chip timing and carrier phase errors in a slowly fading, multipath channel is derived. The receiver is assumed to be a coherent RAKE receiver. Three types of diversity schemes are considered: selection diversity, equal gain diversity combining and maximal ratio diversity combining. The error probability derivation does not resort to the widely used Gaussian approximation for the inter-symbol interference and multiple access interference and is very accurate. The derived series for probability of error calculations is used to assess the reduction in the system capacity due to different levels of synchronization errors. For all three diversity combining schemes considered, the degradation in the system performance is expressed as an effective reduction in the system processing gain. Systems of 1.25MHz, 5MHz and 10MHz are considered for different number of diversity branches and it is shown that the percentage reduction in the system capacity due to synchronization errors is approximately the same for all these systems.

† This research was supported by a grant from the Canadian Institute for Telecommunications Research under the NCE program of the Government of Canada.

‡ M. Oğuz Sunay was with the Department of Electrical and Computer Engineering, Queen's University, Kingston, Ontario, K7L 3N6, Canada. He is now a Member of Technical Staff in Bell Laboratories in Whippany, New Jersey, 07981, USA. Peter J. McLane is with the Department of Electrical and Computer Engineering, Queen's University, Kingston, Ontario, K7L 3N6, Canada.

I Introduction

Direct-sequence code division multiple access (DS CDMA), which was primarily used in military communications until the late 80's, has for some time been the center of attention in cellular radio communications [1-3]. In fact, Europe, Japan and Korea as well as North America have all decided to base at least one of their third generation wireless standards on the DS CDMA technology [4].

In DS CDMA systems, bandwidth spreading is accomplished by direct modulation of a data modulated carrier by a wideband spreading code. Here, the signals all occupy the full allocated bandwidth at all times. Interferers are therefore assumed to come from all directions. The correlation properties of the spreading codes of different users provide multiple access interference immunity in an ideal channel.

In mobile radio environments, the received signals are subjected to multipath fading which severely degrades the system performance. If the system bandwidth is larger than the coherence bandwidth of the channel, fading is frequency selective [5]. In this case, the multipath components in the received signal are resolvable with a resolution in the time delay of T_c, the chip duration. With CDMA techniques, the resolvable paths can be demodulated individually by a RAKE receiver which exploits the excess redundancy due to the presence of independent channel outputs from the multipaths. In a RAKE receiver, information obtained from each branch is combined in a certain way to minimize the interference and further mitigate the fading [6].

The performance of a DS CDMA system is usually measured in terms of the bit error rate as a function of the number of active users for a given signal to noise ratio (SNR). There have been a number of papers on the calculation of error probabilities for DS CDMA systems in the recent literature for both additive white Gaussian noise channels and multipath fading channels [7-14]. Most of these papers use Gaussian approximations for intersymbol interference and multiple access interference and assume that the systems in question enjoy perfect synchronization of the chip timing and the carrier phase. We have previously developed an accurate, infinite series expression for the calculation of error probabilities for a DS CDMA system that uses coherent reception in an AWGN channel without making use of a Gaussian approximation for the interference [16-19]. Furthermore, we did not neglect the presence of synchronization errors in our derivation. In this paper, extending on the procedure of [19], we present a performance analysis technique for a DS CDMA system in a slowly fading multipath environment. We assume that the system uses coherent reception with a RAKE receiver. We consider three different diversity combining schemes, namely, selection diversity, equal gain combining and maximal ratio combining. As in [17-19], we do not neglect the presence of synchronization errors in the system but rather investigate the degradation in the system capacity due to such errors. We show that a synchronization error for such systems can be represented as an effective loss in the processing gain.

An outline of the paper is as follows. The system-fading and multipath model is described in Section II. Section III presents the coherent RAKE receiver and Section IV outlines the use of the Fourier series to develop the infinite series for the bit error rate calculations. The system sensitivity to synchronization errors is discussed in Section V. Finally, conclusions are drawn in Section VI.

II System Model

This paper is concerned with the calculation of the probability of symbol error for a DS CDMA system in a frequency-selective multipath fading environment where each resolvable path is independently Rayleigh faded. The DS CDMA system model examined in this paper is similar to that used in [7] and [8] and is illustrated in Figure 1. Referring to this figure, let us assume that there are K users transmitting signals in the system. Then, each transmitter will transmit a signal in the form,

$$s_k(t) = \sqrt{2P_k} b_k(t - \mathcal{T}_k) a_k(t - \mathcal{T}_k) \cos(\omega_c t + \theta_k) \tag{1}$$

where ω_c is the common signaling frequency, $\mathcal{T}_k$ is the initial message starting times, θ_k is the initial phase offsets and $a_k(t)$ and $b_k(t)$ are the user specific data and spreading signals, respectively. The power of the transmitted signal, $s_k(t)$ can be calculated as

$$\wp_k = \lim_{T\to\infty} \frac{1}{2T} \int_{-T}^{T} |s_k(t)|^2 dt = \lim_{T\to\infty} \frac{1}{T} P_k \left[T + \frac{1}{2w_c} \sin(2w_c T + 2\theta_k) \right] = P_k. \tag{2}$$

The data modulation $a_k(t)$ is a sequence of nonoverlapping rectangular pulses of duration T, each of which has an amplitude of 1 or -1 with equal probability. Mathematically $a_k(t)$ can be represented as,

$$a_k(t) = \sum_{i=-\infty}^{\infty} a_{k,i} \cdot p_T(t - iT). \tag{3}$$

Here, $a_{k,i}$ is one symbol of the data modulation and takes on values $\{\mp 1\}$ randomly and $p_T(t)$ is the rectangular pulse of duration T. Similarly, the long PN sequence $b_k(t)$ has the form,

$$b_k(t) = \sum_{i=-\infty}^{\infty} b_{k,i} \cdot \psi(t - iT_c) \tag{4}$$

where $b_{k,i}$ is one chip of the PN sequence and takes on values $\{\mp 1\}$ randomly. The chip waveform $\psi(t)$ has duration $T_c = T/G$ where G is the system processing gain. Note that since the PN sequences are assumed to be long, the period of $b_k(t)$ is much larger than T.

Mobile radio channels are effectively modeled as a continuum of multipath components, and thus the lowpass equivalent impulse response of the channel $h_k(\tau;t)$ can be written as,

$$h_k(\tau;t) = \sum_{l=-\infty}^{\infty} h_{k,l}(t)\delta(\tau - t_{kl}(t)) \tag{5}$$

where the tap gains $h_{k,l}(t)$ are complex Gaussian random variables and the time delays $t_{kl}(t)$ are uniformly distributed over the interval $[0,T]$ [23, 24]. When a wide-sense stationary channel with uncorrelated scattering is considered, $h_{k,l}(t)$ are independent, identically distributed random variables since they are modeled to have Gaussian distributions [27]. For a multipath delay spread of T_m, (5) can be truncated at $L = \left\lfloor \frac{T_m}{T_c} \right\rfloor + 1$ [5]. Here $\lfloor x \rfloor$ denotes the largest integer that is less than or equal to x. For a slowly varying channel, one can assume that $h_{k,l}(t) = h_{k,l}$ and $t_{kl}(t) = t_{kl}$ during at least an entire duration of one symbol. Since $h_{k,l}$ are complex Gaussian random variables, the channel model can equivalently be written as,

$$h_k(t) = \sum_{l=1}^{L} \beta_{kl} \exp\{j\vartheta_{kl}\}\delta(t - t_{kl}) \tag{6}$$

where β_{kl} is the path gain, ϑ_{kl} and t_{kl} are the phase and time offsets introduced by the multipath channel on the l'th path of the k'th user's signal. In this case, $\beta_{k,l}$ is Rayleigh distributed with $\mathrm{E}\{\beta_{kl}^2\} = 2\rho_0$ and has a probability density function

$$f_{\beta_{kl}}(x) = \frac{x}{\rho_0} \exp\left(-\frac{x^2}{2\rho_0}\right) u(x) \tag{7}$$

where $u(x)$ is the unit step function. Note that the frequency-nonselective channel is a special case of the channel described by (6) with $L = 1$.

The total received signal can then be written as,

$$r(t) \;=\; \sum_{k=1}^{K} \int_{-\infty}^{\infty} h_k(\varphi) s_k(t - \varphi) d\varphi + n(t)$$

$$= \sum_{k=1}^{K} \sum_{l=1}^{L} \sqrt{2P_k}\beta_{kl} b_k(t - \mathcal{T}_k - t_{kl}) a_k(t - \mathcal{T}_k - t_{kl}) \cos(\omega_c t + \theta_k + \vartheta_{kl} - \omega_c \tau_{kl}) + n(t) \quad (8)$$

where $n(t)$ is the additive white Gaussian noise (AWGN) introduced by the channel. The net time delay, τ_{kl}, and the net phase offset, ϕ_{kl}, are obtained by summing their respective transmitter and channel parts such that,

$$\tau_{kl} = \mathcal{T}_k + t_{kl}, \quad (9)$$

$$\phi_{kl} = \theta_k + \vartheta_{kl} - \omega_c \tau_{kl}. \quad (10)$$

The distributions of the random variables τ_{kl} and ϕ_{kl} are discussed in the next section for all values of k and l.

III Receiver Model

We want to capture the signal from user 1, namely, $a_1(t)$. The received signal goes through a RAKE receiver as shown in Figure 2. Here, the received signal is despread independently for each multipath component by multiplying the spreading code of the first user delayed by an amount equal to the delay of the multipath component. The signal is then stripped off its carrier and passed through a bank of correlators.

For the analysis, we consider a data symbol interval as $[0, T]$ for convenience. In this case, from Figure 2, the input to the decision device from the j'th path is,

$$\begin{aligned} Z_{1j} &= 2\int_{\hat{\tau}_{1j}}^{T+\hat{\tau}_{1j}} b_1(t - \hat{\tau}_{1j}) r(t) \cos(2\pi f_c t + \hat{\phi}_{1j}) dt \\ &= D_{1j} + I_{1j} + M_{1j} + N_{1j} \end{aligned} \quad (11)$$

where $\hat{\tau}_{1j}$ and $\hat{\phi}_{1j}$ are the estimates of τ_{1j} and ϕ_{1j}, respectively. In (11), D_{1j}, I_{1j}, M_{1j} and N_{1j} correspond to the terms that consist of the desired signal plus self interference caused by synchronization errors, intersymbol interference caused by multipath, multiple access interference and additive white Gaussian noise, respectively. These terms can be expressed as,

$$D_{1j} = \sqrt{2P_1}\beta_{1j} \cos(\phi_{1j} - \hat{\phi}_{1j}) \int_{\hat{\tau}_{1j}}^{T+\hat{\tau}_{1j}} b_1(t - \hat{\tau}_{1j}) b_1(t - \tau_{1j}) a_1(t - \tau_{1j}) dt, \quad (12)$$

$$
\begin{aligned}
I_{1j} &= \sum_{\substack{l=1\\l\neq j}}^{L} \sqrt{2P_1}\beta_{1l}\cos(\phi_{1l}-\hat{\phi}_{1j})\int_{\hat{\tau}_{1j}}^{T+\hat{\tau}_{1j}} b_1(t-\hat{\tau}_{1j})b_1(t-\tau_{1l})a_1(t-\tau_{1l})dt, & (13)\\
M_{1j} &= \sum_{k=2}^{K}\sum_{l=1}^{L} \sqrt{2P_1}\beta_{kl}\cos(\phi_{kl}-\hat{\phi}_{1j})\int_{\hat{\tau}_{1j}}^{T+\hat{\tau}_{1j}} b_1(t-\hat{\tau}_{1j})b_k(t-\tau_{kl})a_k(t-\tau_{kl})dt, & (14)\\
& & (15)
\end{aligned}
$$

and

$$
N_{1j} = 2\int_{\hat{\tau}_{1j}}^{T+\hat{\tau}_{1j}} n(t)b_1(t-\hat{\tau}_{1j})\cos(2\pi f_c t+\hat{\phi}_{1j})dt. \qquad (16)
$$

A system with synchronization errors will not be able to estimate the time delays and phase delays corresponding to the individual paths in the RAKE receiver correctly. The chip timing and carrier phase errors for the j'th path will be, $\tau_{1j}-\hat{\tau}_{1j}$ and $\phi_{1j}-\hat{\phi}_{1j}$, respectively. Without any loss of generality, we assume that $\hat{\tau}_{1j}=\hat{\phi}_{1j}=0$. Then, for our purposes, τ_{1j} and ϕ_{1j} are the chip timing and carrier phase errors, respectively.

We now simplify D_{1j}. Using (3), (12) can be rewritten as,

$$
\begin{aligned}
D_{1j} &= \sqrt{2P_1}\beta_{1j}\cos(\phi_{1j})a_{1,-1}\int_0^{\tau_{1j}} b_1(t)b_1(t-\tau_{1j})dt\\
&\quad +\sqrt{2P_1}\beta_{1j}\cos(\phi_{1j})a_{1,0}\int_{\tau_{1j}}^{T} b_1(t)b_1(t-\tau_{1j})dt. \qquad (17)
\end{aligned}
$$

Now, using the following partial correlation functions defined in the literature by Pursley [26],

$$
\begin{aligned}
R_{ij}(\tau) &= \int_0^{\tau} b_i(t)b_j(t-\tau)dt, & (18)\\
\hat{R}_{ij}(\tau) &= \int_{\tau}^{T} b_i(t)b_j(t-\tau)dt & (19)
\end{aligned}
$$

we can rewrite (17) as,

$$
\begin{aligned}
D_{1j} &= \sqrt{2P_1}\beta_{1j}\cos(\phi_{1j})a_{1,-1}b_{1,0}b_{1,-1}R_{11}(\tau_{1j})\\
&\quad +\sqrt{2P_1}\beta_{1j}\cos(\phi_{1j})a_{1,0}\hat{R}_{11}(\tau_{1j}) \qquad (20)
\end{aligned}
$$

For random PN sequences with rectangular shaped chips it is possible to further simplify (20). By making use of (4) and the fact that $|\tau_{1j}|<T_c$ in order for the spread spectrum system to successfully operate, we get,

$$
D_{1j} = \sqrt{2P_1}\beta_{1j}\cos(\phi_{1j})a_{1,-1}b_{1,0}b_{1,-1}\tau_{1j}
$$

$$+\sqrt{2P_1}\beta_{1j}\cos(\phi_{1j})a_{1,0}G(T_c-\tau_{1j})$$
$$+\sqrt{2P_1}\beta_{1j}\cos(\phi_{1j})a_{1,0}\sum_{m=1}^{G-1} b_{1,m}b_{1,(m-1)}\tau_{1j}. \tag{21}$$

We define the following random variables,

$$\alpha_0 \triangleq a_{1,-1}b_{1,0}b_{1,-1}, \tag{22}$$
$$\alpha_i \triangleq a_{1,0}b_{1,i}b_{1,(i-1)}, \qquad i=1,2,\ldots,G-1. \tag{23}$$

Then, $\alpha_i, i=0,\ldots,(G-1)$ are iid random variables taking on values $\{\mp 1\}$ with equal probability. Thus (21) can be rewritten as,

$$D_{1j} = D_{1ja} + D_{1jb} \tag{24}$$

where

$$D_{1ja} = \sqrt{2P_1}\beta_{1j}\cos(\phi_{1j})G(T_c-\tau_{1j})a_{1,0} \tag{25}$$

and

$$D_{1jb} = \sqrt{2P_1}\beta_{1j}\cos(\phi_{1j})\tau_{1j}\sum_{m=0}^{G-1}\alpha_m. \tag{26}$$

Here, D_{1ja} is the desired signal term and D_{1jb} is the self interference term caused by the non-zero chip timing error. Note that if the system is free of synchronization errors,

$$D_{1ja} = \sqrt{2P_1}\beta_{1j}Ta_{1,0}, \tag{27}$$
$$D_{1jb} = 0. \tag{28}$$

Now, we simplify the intersymbol interference term, I_{1j}, defined in (13). Once again, using (2) and (3), (13) can be rewritten as,

$$I_{1j} = \sum_{\substack{l=1\\ l\neq j}}^{L} \sqrt{2P_1}\beta_{1l}\cos(\phi_{1l})\left[a_{1,-1}R_{11}(\tau_{1l}) + a_{1,0}\hat{R}_{11}(\tau_{1l})\right]. \tag{29}$$

where $\tau_{1l}, l\neq j$ are modeled to be iid random variables, uniformly distributed over $[0,T_m]$ where T_m is the multipath delay spread of the channel. Similarly, we model ϕ_{1l} to be iid random variables, uniform in $[0,2\pi]$. Then, the autocorrelation functions in (29) can easily be evaluated. We define $\Delta t_{1l} = \tau_{1l} \mod T_c$ and $R = (\tau_{1l} - \Delta t_{1l})/T_c$. In this case, Δt_{1l} is a random variable that has a probability density function (pdf) dependent on the specific value of the maximum multipath delay spread, T_m. If T_m is an integer multiple of the chip duration, T_c, Δt_{1l} is uniform in $[0, T_c]$. Otherwise, the pdf of Δt_{1l} will see a drop in its value in the interval $[T_m \bmod T_c, T_c]$ and correspondingly, the pdf value in the interval $[0, T_m \bmod T_c]$ will increase as shown in Figure 3. This deviation from the uniform distribution will be negligibly small since $T_m >> T_c$, and hence, for our purposes, we assume that Δt_{1l} is uniformly distributed in $[0, T_c]$. We also define two random variables $\xi_{li} = b_{1,i} b_{1,x}$ and $\gamma_{li} = b_{1,i} b_{1,(x-1)}$ where x is an integer number that is dependent on the value of τ_{1l}. Regardless of the value of x, however, ξ_{li} and γ_{li} are iid random variables taking on the values $\{\mp 1\}$ randomly. Then,

$$\begin{aligned} R_{11}(\tau_{1l}) &= \sum_{i=0}^{R-1} \left[\gamma_{li} \Delta t_{1l} + \xi_{li}(T_c - \Delta t_{1l})\right] + \gamma_{lR} \Delta t_{1l} && (30) \\ \hat{R}_{11}(\tau_{1l}) &= \xi_{lR}(T_c - \Delta t_{1l}) + \sum_{i=R+1}^{G-1} \left[\gamma_{li} \Delta t_{1l} + \xi_{li}(T_c - \Delta t_{1l})\right] && (31) \end{aligned}$$

We now define the following random variables,

$$\begin{aligned} \tilde{\alpha}_{li} &= \begin{cases} a_{1,-1}\xi_{li} & i = 0, \ldots, R \\ a_{1,0}\xi_{li} & i = R+1, \ldots, G-1 \end{cases} \\ \underline{\alpha}_{li} &= \begin{cases} a_{1,-1}\gamma_{li} & i = 0, \ldots, R-1 \\ a_{1,0}\gamma_{li} & i = R, \ldots, G-1 \end{cases} \end{aligned}$$

$\tilde{\alpha}_{li}$ and $\underline{\alpha}_{li}$ are iid random variables that take on values $\{\mp 1\}$ randomly. Then,

$$I_{1j} = \sum_{\substack{l=1 \\ l \neq j}}^{L} \sum_{i=0}^{G-1} \sqrt{2P_1}\beta_{1l}\cos(\phi_{1l})\left[\Delta t_{1l}\tilde{\alpha}_{li} + (T_c - \Delta t_{1l})\underline{\alpha}_{li}\right] \tag{32}$$

Now, we simplify the multiple access interference term, M_{1j}, defined in (14). For all practical reasons, all of the information signals that cause interference may be considered to be random and thus be imbedded into the long PN sequences. Thus we define,

$$q_k(t) = a_k(t) b_k(t) = \sum_{i=-\infty}^{\infty} q_{k,i}\psi(t - iT_c) \tag{33}$$

where, for our purposes, $q_{k,i}$ is a set of random variables that randomly take on the values $\{\mp 1\}$. Then, without any loss of generality, the random variables $\tau_{kl}, k = 2, \ldots, K$ can be assumed to be iid and uniformly distributed over the interval $[0, T_c]$. The random variables,

ϕ_{kl} are assumed to be iid and uniform over $[0, 2\pi]$. Therefore we get,

$$\begin{aligned} M_{1j} &= \sum_{k=2}^{K}\sum_{l=1}^{L}\sqrt{2P_k}\beta_{kl}\cos(\phi_{kl})\sum_{j=0}^{G-1}\int_{jT_c}^{(j+1)T_c} b_{1,j}\sum_{i=-\infty}^{\infty} q_{k,i}\psi(t-jT_c)\psi(t-iT_c-\tau_{kl})dt \\ &= \sum_{k=2}^{K}\sum_{l=1}^{L}\sum_{j=0}^{G-1}\sqrt{2P_k}\beta_{kl}\cos(\phi_{kl})\left[b_{1,j}q_{k,(j-1)}\tau_{kl} + b_{1,j}q_{k,j}(T_c-\tau_{kl})\right]. \end{aligned} \quad (34)$$

We now define the following random variables,

$$\begin{aligned} \eta_{kj} &= b_{1,j}q_{k,(j-1)} \\ \kappa_{kj} &= b_{1,j}q_{k,j} \end{aligned}$$

Then, η_{kj} and κ_{kj} are iid random variables that take on values $\{\mp 1\}$ randomly. Thus,

$$M_{1j} = \sum_{k=2}^{K}\sum_{l=1}^{L}\sum_{j=0}^{G-1}\sqrt{2P_k}\beta_{kl}\cos(\phi_{kl})\left[\eta_{kj}\tau_{kl} + \kappa_{kj}(T_c-\tau_{kl})\right] \quad (35)$$

Finally, the AWGN term, N_{1j} is a Gaussian random variable with zero mean and N_0T variance [27].

IV Bit Error Rate Analysis

Suppose that $a_{1,0} = 1$ represents the binary symbol 1 and $a_{1,0} = -1$ represents the binary symbol 0. The decision device in Figure 2 produces the symbol 1 if the decision variable $Z > 0$ and the symbol 0 if $Z < 0$. An error occurs if $Z < 0$ when $a_{1,0} = 1$ or if $Z > 0$ when $a_{1,0} = -1$. Since $a_{1,0}$ is assumed to take on values $\{\mp 1\}$ with equal probability, the probability of error is simply equal to the probability of having $Z > 0$ when $a_{1,0} = -1$,

$$P(E) = P(Z > 0 | a_{1,0} = -1). \quad (36)$$

Recall from (11) and (24) that the input signal to the decision device from the j'th path of the receiver is $Z_{1j} = D_{1ja} + D_{1jb} + I_{1j} + M_{1j} + N_{1j}$ where D_{1ja} is the desired signal, D_{1jb} is the self interference due to chip timing errors, I_{1j} is the intersymbol interference due to the multipath, M_{1j} is the multiple access interference and N_{1j} is the AWGN term with zero mean and N_0T variance.

Once all Z_{1j}'s are obtained, diversity combining is performed in the receiver and the decision variable Z is formed. We consider three diversity combining schemes: selection diversity, maximal ratio diversity combining and equal gain diversity combining.

IV.1 Selection Diversity

When selection diversity is employed, the receiver simply selects the receiver path with the highest path gain, β_{1j}, and uses the information from this path to estimate the transmitted signal $a_1(t)$. The other paths are not used in the decision making process. In other words, the decision variable Z is equal to,

$$Z = \mathrm{Max}_{\beta_{1j}}\{Z_{1j}\}. \tag{37}$$

Since only the j'th path is used in the decision making, the chip timing and carrier phase errors in the receiver are, τ_{1j} and ϕ_{1j}, respectively. When the j'th path gain is the maximum of the L gains where the individual gains are Rayleigh distributed, the probability density function of the j'th path gain will be in the form,

$$f_{\beta_{1j}}(x) = L \sum_{k=0}^{L-1} \binom{L-1}{k} \frac{(-1)^k x}{\rho_0} \exp\left(-\frac{x^2(k+1)}{2\rho_0}\right) u(x) \tag{38}$$

as shown in equation (5.2-7) of [23].

The error probability conditioned on the random variables $I_{1j}, M_{1j}, \beta_{1j}$ and α_m is,

$$P(E|I_{1j}, M_{1j}, \beta_{1j}, \alpha_m) = Q\left[\frac{\sqrt{2P_1}\beta_{1j}\cos(\phi_{1j})\left((T_c - \tau_{1j})G - \tau_{1j}\sum_{m=0}^{G-1}\alpha_m\right) - I_{1j} - M_{1j}}{\sqrt{N_0 T}}\right] \tag{39}$$

where $Q(x)$ is the Q-function defined as,

$$Q(x) = \int_x^\infty \frac{e^{-t^2/2}}{\sqrt{2\pi}} dt. \tag{40}$$

The random variables I_{1j} and M_{1j} all arise from different phyisical sources. Hence they are independent. Thus, using the total probability theorem [27], the error probability conditioned only on β_{1j} and α_m is written as,

$$P(E|\beta_{1j}, \alpha_m) = \int_{-\infty}^{\infty}\int_{-\infty}^{\infty} P(E|I_{1j}, M_{1j}, \beta_{1j}, \alpha_m) f_{I_{1j}}(i) f_{M_{1j}}(m)\ di\ dm \tag{41}$$

The probability density functions $f_{I_{1j}}(i)$ and $f_{M_{1j}}(m)$ are difficult to determine. Instead, we proceed to rewrite the conditional error probability given in (39) using a Fourier series expansion of $Q(x)$ [22]. We define the error function $Q(x)$ to be,

$$Q(x) \simeq \sum_{m=-\infty}^{\infty} c_m e^{jm\omega x} \tag{42}$$

where ω is the Fourier series frequency and c_m are the Fourier series coefficients and are given by,

$$c_m = \begin{cases} \frac{1}{j2m} e^{-m^2\omega^2/2} & m > 0 \text{ and } m \text{ odd} \\ 0 & m > 0 \text{ and } m \text{ even} \\ \frac{1}{2} & m = 0 \end{cases} \tag{43}$$

with $c_{-m} = -c_m, m > 0$ [22]. (42) becomes exact in the limit as w goes to zero.

If we substitute (42) into (41), we obtain,

$$\begin{aligned} P(E|\beta_{1j}, \alpha_m) &= \sum_{m=-\infty}^{\infty} c_m e^{\frac{jm\omega\sqrt{2P_1}\beta_{1j}\cos(\phi_{1j})\left((T_c-\tau_{1j})G-\tau_{1j}\sum_{m=0}^{G-1}\alpha_m\right)}{\sqrt{N_0T}}} \\ &\quad \cdot \int_{-\infty}^{\infty}\int_{-\infty}^{\infty} e^{-jm\omega\frac{i+m}{\sqrt{N_0T}}} f_{I_{1j}}(i) f_{M_{1j}}(m)\ di\ dm. \end{aligned} \tag{44}$$

But, the characteristic function of a random variable, P is defined as,

$$\Phi_P(\omega) = \mathrm{E}\{\exp(j\omega P)\} = \int_{-\infty}^{\infty} e^{j\omega p} f_P(p)\ dp. \tag{45}$$

Then,

$$\begin{aligned} P(E|\beta_{1j}, \alpha_m) &= \sum_{m=-\infty}^{\infty} c_m e^{\frac{jm\omega\sqrt{2P_1}\beta_{1j}\cos(\phi_{1j})\left((T_c-\tau_{1j})G-\tau_{1j}\sum_{m=0}^{G-1}\alpha_m\right)}{\sqrt{N_0T}}} \\ &\quad \cdot \Phi_{I_{1j}}\left(-\frac{m\omega}{\sqrt{N_0T}}\right) \cdot \Phi_{M_{1j}}\left(-\frac{m\omega}{\sqrt{N_0T}}\right) \end{aligned} \tag{46}$$

Thus, we need only to find the characteristic functions of I_{1j} and M_{1j}. To this end, we let,

$$i_l = \sqrt{2P_1}\beta_{1l}\cos(\phi_{1l}) \sum_{i=0}^{G-1} \left[\Delta t_{1l}\tilde{\alpha}_i + (T_c - \Delta t_{1l})\underline{\alpha}_i\right] \tag{47}$$

to get

$$I_{1j} = \sum_{\substack{l=1 \\ l\neq j}}^{L} i_l. \tag{48}$$

Since the i_l are independent random variables,

$$\Phi_{I_{1j}}(\omega) = [\Phi_{i_l}(\omega)]^{L-1} \tag{49}$$

If (47) is studied, it is seen that the random variables β_{1l}, ϕ_{1l} and Δt_{1l} remain constant throughout the duration of G chips whereas the random variables $\tilde{\alpha}_i$ and $\underline{\alpha}_i$ vary independently from chip to chip. In this case, the characteristic function of i_l is defined as,

$$\begin{aligned} \Phi_{i_l}(\omega) &= \mathrm{E}\left\{e^{j\omega\sqrt{2P_1}\beta_{1l}\cos(\phi_{1l})\sum_{i=0}^{G-1}\left[\Delta t_{1l}\tilde{\alpha}_i + (T_c-\Delta t_{1l})\underline{\alpha}_i\right]}\right\} \\ &= \mathrm{E}\left\{\left[\cos(\omega\sqrt{2P_1}\beta_{1l}\cos(\phi_{1l})T_c) + \cos(\omega\sqrt{2P_1}\beta_{1l}\cos(\phi_{1l})(2\Delta t_{1l} - T_c))\right]^G\right\} \end{aligned} \tag{50}$$

Using the binomial expansion, it is possible to rewrite (50) as,

$$\Phi_{i_l}(\omega) = \mathrm{E}\left\{\sum_{p=0}^{G}\binom{G}{p}\cos^p(\omega\sqrt{2P_1}\beta_{1l}\cos(\phi_{1l})(2\Delta t_{1l}-T_c))\cos^{G-p}(\omega\sqrt{2P_1}\beta_{1l}\cos(\phi_{1l})T_c)\right\} \quad (51)$$

It is possible to perform the expectation on the random variable Δt_{1l} analytically. Using (2.513.3) and (2.513.4) on page 132 of [28], we get,

$$\begin{aligned}\Phi_{i_l}(\omega) &= \mathrm{E}\left\{\sum_{p=0}^{G/2}\binom{G}{2p}\binom{2p}{p}\frac{\cos^{G-2p}(\omega\sqrt{2P_1}\beta_{1l}\cos(\phi_{1l})T_c)}{2^{2p}}\right.\\ &\quad +\sum_{p=1}^{G}\binom{G}{p}\frac{\cos^{G-p}(\omega\sqrt{2P_1}\beta_{1l}\cos(\phi_{1l})T_c)}{2^{p-1}\omega\sqrt{2P_1}\beta_{1l}\cos(\phi_{1l})T_c}\\ &\quad \left.\cdot\sum_{q=0}^{\lfloor\frac{p-1}{2}\rfloor}\binom{p}{q}\frac{\sin((p-2q)\omega\sqrt{2P_1}\beta_{1l}\cos(\phi_{1l})T_c)}{p-2q}\right\}. \end{aligned} \quad (52)$$

The expectation relative to the random variables β_{1l} and ϕ_{1l} can be performed using numerical integration. A simple trapezoidal rule provides accurate results in a reasonably fast manner. Once the numerical integration is performed, the characteristic function of I_{1j} can simply be found using (49).

We now find the characteristic function of M_{1j}. To this end, we let,

$$m_{kl} = \sqrt{2P_k}\beta_{kl}\cos(\phi_{kl})\sum_{j=0}^{G-1}\left[\eta_{kj}\tau_{kl}+\kappa_{kj}(T_c-\tau_{kl})\right]. \quad (53)$$

to get

$$M_{1j} = \sum_{k=2}^{K}\sum_{l=1}^{L} m_{kl}. \quad (54)$$

Similar to i_l in (48), the m_{kl} are iid random variables as well. Therefore,

$$\Phi_{M_{1j}}(\omega) = \left[\Phi_{m_{kl}}(\omega)\right]^{(K-1)L} \quad (55)$$

where the characteristic function of m_{kl} is found as,

$$\begin{aligned}\Phi_{m_{kl}}(\omega) &= \mathrm{E}\left\{e^{j\omega\sqrt{2P_k}\beta_{kl}\cos(\phi_{kl})\sum_{j=0}^{G-1}\left[\eta_{kj}\tau_{kl}+\kappa_{kj}(T_c-\tau_{kl})\right]}\right\}\\ &= \mathrm{E}\left\{\left[\cos(\omega\sqrt{2P_k}\beta_{kl}\cos(\phi_{kl})T_c)+\cos(\omega\sqrt{2P_k}\beta_{kl}\cos(\phi_{kl})(2\tau_{kl}-T_c))\right]^G\right\}\end{aligned}$$

$$
\begin{aligned}
= \quad & \mathrm{E}\left\{\sum_{p=0}^{G}\binom{G}{p}\cos^{p}(\omega\sqrt{2P_k}\beta_{kl}\cos(\phi_{kl})(2\tau_{kl}-T_c))\right.\\
& \left.\cdot\cos^{G-p}(\omega\sqrt{2P_k}\beta_{kl}\cos(\phi_{kl})T_c)\right\} \qquad (56)
\end{aligned}
$$

As before, the expectation on the random variable, τ_{kl} can be performed analytically. Using [28] we get,

$$
\begin{aligned}
\Phi_{m_{kl}}(\omega) \quad = \quad & \mathrm{E}\left\{\sum_{p=0}^{G/2}\binom{G}{2p}\binom{2p}{p}\frac{\cos^{G-2p}(\omega\sqrt{2P_k}\beta_{kl}\cos(\phi_{kl})T_c)}{2^{2p}}\right.\\
& +\sum_{p=1}^{G}\binom{G}{p}\frac{\cos^{G-p}(\omega\sqrt{2P_k}\beta_{kl}\cos(\phi_{kl})T_c)}{2^{p-1}\omega\sqrt{2P_k}\beta_{kl}\cos(\phi_{kl})T_c}\\
& \left.\cdot\sum_{q=0}^{\lfloor\frac{p-1}{2}\rfloor}\binom{p}{q}\frac{\sin((p-2q)\omega\sqrt{2P_k}\beta_{kl}\cos(\phi_{kl})T_c)}{p-2q}\right\}. \qquad (57)
\end{aligned}
$$

The expectation relative to the random variables β_{kl} and ϕ_{kl} in equation (46) can be performed using numerical integration. Note that the characteristic functions of i_l and m_{kl} become identical if $P_1 = P_k$. Once again, trapezoidal rule can be used to perform these integrations.

An alternative way to find the characteristic functions of I_{1j} and M_{1j} would be to make some independence assumptions as was done earlier in [19, 18] at the expense of some degradation in the accuracy of the technique. If one assumes that the products $\beta_{1l}\cos(\phi_{1l})[\Delta t_{1l}\tilde{\alpha}_i + (T_c - \Delta t_{1l})\underline{\alpha}_i]$ and $\beta_{kl}\cos(\phi_{kl})\left[\eta_{kj}|\tau_{kl}| + \kappa_{kj}(T_c - |\tau_{kl}|)\right]$ vary independently from chip to chip, it is possible to find closed form expressions for the characteristic functions of I_{1j} and M_{1j} and these expressions would be significantly faster to compute. Under these assumptions we first define,

$$
i_{li} = \sqrt{2P_1}\beta_{1l}\cos(\phi_{1l})\left[\Delta t_{1l}\tilde{\alpha}_i + (T_c - \Delta t_{1l})\underline{\alpha}_i\right] \qquad (58)
$$

to get

$$
I_{1j} = \sum_{\substack{l=1 \\ l\neq j}}^{L}\sum_{i=0}^{G-1} i_{li}. \qquad (59)
$$

and since i_{li} are assumed to be iid, this would result in,

$$
\Phi_{I_{1j}}(\omega) = \left[\Phi_{i_{li}}(\omega)\right]^{G(L-1)}. \qquad (60)
$$

Thus, we find the characteristic function of i_{li}. By using the equations (9.1.18) on page 360 of [29] and (6.629) on page 716 of [28] we get,

$$\begin{aligned}\Phi_{i_{li}}(\omega) &= \mathrm{E}\{\frac{1}{2}J_0(\omega\sqrt{2P_1}\beta_{1l}T_c) + \frac{1}{2}J_0(\omega\sqrt{2P_1}\beta_{1l}(2\Delta t_{1l} - T_c))\} \\ &= \frac{1}{2}e^{-\omega^2 P_1 \rho_0 T_c^2} \\ &\quad + \frac{1}{2}\sum_{n=0}^{\infty} \frac{n!(\omega\sqrt{P_1\rho_0}T_c)^{2n}}{(2n+1)!} M(n+1, 2(n+1), -\omega^2 P_1 \rho_0 T_c^2) \end{aligned} \tag{61}$$

where $J_0(x)$ is the zeroth order Bessel function and $M(a, b, z)$ is the confluent hypergeometric function and is defined as,

$$M(a, b, z) = \sum_{k=0}^{\infty} \frac{(a)_k z^k}{(b)_k k!} \tag{62}$$

where $(a)_0 = 1$ and $(a)_n = a(a+1)\ldots(a+n-1)$ [29]. Note that (61) is in its closed form and does not require numerical integration. Once (61) is computed, the characteristic function of I_{1j} can easily be found using (60).

We continue with the derivation of the characteristic function for the multiple access interference term, M_{1j}. For this purpose we define,

$$m_{klj} = \sqrt{2P_k}\beta_{kl}\cos(\phi_{kl})\left[\eta_{kj}\tau_{kl} + \kappa_{kj}(T_c - \tau_{kl})\right]. \tag{63}$$

From (29),

$$M_{1j} = \sum_{k=2}^{K}\sum_{l=1}^{L}\sum_{j=0}^{G-1} m_{klj} \tag{64}$$

Once again, using the equations (9.1.18) on page 360 of [29] and (6.629) on page 716 of [28] we get,

$$\begin{aligned}\Phi_{m_{klj}}(\omega) &= \mathrm{E}\left\{\frac{1}{2}J_0(\omega\sqrt{2P_k}\beta_{kl}T_c) + \frac{1}{2}J_0(\omega\sqrt{2P_k}\beta_{kl}(2\tau_{kl} - T_c))\right\} \\ &= \frac{1}{2}e^{-\omega^2 P_k \rho_0 T_c^2} \\ &\quad + \frac{1}{2}\sum_{n=0}^{\infty} \frac{n!(\omega\sqrt{P_k\rho_0}T_c)^{2n}}{(2n+1)!} M(n+1, 2(n+1), -\omega^2 P_k \rho_0 T_c^2) \end{aligned} \tag{65}$$

and since m_{klj} are iid random variables, from (64),

$$\Phi_{M_{1j}}(\omega) = \prod_{k=2}^{K}\prod_{l=1}^{L}\prod_{j=0}^{G-1} \Phi_{m_{klj}}(\omega) \tag{66}$$

Having found the expressions for the characteristic functions of I_{1j} and M_{1j}, we can now find the infinite series for the error probability. Using (43) and (46),

$$\begin{aligned} P(E|\beta_{1j}, \alpha_m) &= \frac{1}{2} - \frac{2}{\pi} \sum_{\substack{m=1 \\ m \mathrm{odd}}}^{\infty} \frac{1}{m} e^{-m^2\omega^2/2} \\ &\quad \cdot \sin\left(\frac{m\omega\sqrt{2P_1}\beta_{1j}\cos(\phi_{1j})\left((T_c - |\tau_{1j}|)G - |\tau_{1j}|\sum_{m=0}^{G-1}\alpha_m\right)}{\sqrt{N_0 T}} \right) \\ &\quad \cdot \Phi_I(-\frac{m\omega}{\sqrt{N_0 T}}) \cdot \Phi_M(-\frac{m\omega}{\sqrt{N_0 T}}) \end{aligned} \tag{67}$$

where the characteristic functions of I_{1j} and M_{1j} can be found using either (49) and (55) or (60) and (66). We need to integrate $P(E)$ over the distributions of β_{1j} and $\alpha_m, m = 0, \ldots, G-1$ to get the unconditional error probability expression. Recall that when selection diversity is employed β_{1j} has a probability density function of the form given in (38). α_m, on the other hand, are iid random variables that take on values $\{\mp 1\}$ randomly. We define,

$$\alpha = \sum_{m=0}^{G-1} \alpha_m. \tag{68}$$

Then, α is a random variable with binomial distribution. Since β_{1j} and α are independent random variables,

$$P(E) = \int_{-\infty}^{\infty}\int_{-\infty}^{\infty} P(E|\beta_{1j}, \alpha) f_{\beta_{1j}}(y) f_\alpha(x)\, dy\, dx \tag{69}$$

By using equations (3.952.1) on page 495, (3.323.2) on page 307 and (3.462.6) on page 338 of [28] successively and performing some substitutions we get,

$$\begin{aligned} P(E) &= \frac{1}{2} - \frac{2}{\pi} \sum_{\substack{m=1 \\ m \text{ odd}}}^{\infty} \frac{1}{m} e^{-m^2\omega^2/2} L \sum_{k=0}^{L-1} \binom{L-1}{k} \frac{(-1)^k C_{mk}}{k+1} \sqrt{\frac{\pi}{D_{mk}^2 + 1/(2G)}} \\ &\quad \cdot \left(1 - \frac{D_{mk}^2}{D_{mk}^2 + 1/(2G)}\right) \exp\left\{ \frac{C_{mk}^2 D_{mk}^2}{D_{mk}^2 + 1/(2G)} - C_{mk}^2 \right\} \frac{1}{\sqrt{2G}} \\ &\quad \cdot \Phi_{I_{1j}}(-\frac{m\omega}{\sqrt{N_0 T}}) \cdot \Phi_{M_{1j}}(-\frac{m\omega}{\sqrt{N_0 T}}) \end{aligned} \tag{70}$$

where

$$C_{mk} = \frac{m\omega\sqrt{2P_1}\cos(\phi_{1j})(T_c - |\tau_{1j}|)G}{2\sqrt{N_0 T}\left(\frac{k+1}{2\rho_0}\right)^{1/2}}, \tag{71}$$

$$D_{mk} = \frac{m\omega\sqrt{2P_1}\cos(\phi_{1j})|\tau_{1j}|}{2\sqrt{N_0 T}\left(\frac{k+1}{2\rho_0}\right)^{1/2}}. \tag{72}$$

We use both methods of finding the characteristic functions for the interference terms to compute the system capacities at different chip timing and carrier phase errors. System performance as a function of the number of active users is graphed for both methods in Figure 4 for systems at various synchronization error levels. Here, systems with 2 multipaths and 20dB SNR are considered. As can be seen from Figure 4, the probability of error calculated from the two methods is slightly different; the independence assumption results in slightly optimistic values. The difference, however, is never large enough to grant a discrepency in the system capacity calculated using these methods. We find that when an error probability of 10^{-3} is desired, the two methods give exactly same value for the system capacity at all synchronization error levels.

IV.2 Maximal Ratio Combining

When maximal ratio combining is employed, the receiver, having perfect knowledge of the individual path gains, weighs each path with its corresponding path gain and then sums these weighted terms. It is this sum that is used in the decision making. Then,

$$\begin{aligned} Z &= \sum_{j=1}^{L} \beta_{1j} Z_{1j} \\ &= \sum_{j=1}^{L} \beta_{1j} \{D_{1j} + I_{1j} + M_{1j} + N_{1j}\} \\ &= D + I + M + N \end{aligned} \tag{73}$$

where D is the sum of the desired signal terms from all branches, I is the intersymbol interference, M is the multiple access interference and N is the AWGN term with variance equal to,

$$\sigma_N^2 = 2N_0 T \rho_0 L\{1 + (L-1)\frac{\rho_0^2 \pi}{4}\} \tag{74}$$

since $\mathrm{E}\{\beta_{1j}^2\} = 2\rho_0$ and $\mathrm{E}\{\beta_{1j}\} = \rho_0\sqrt{2\pi\rho_0}/2$. Since all of the branches are used in the decision making, each branch in the receiver structure of Figure 2 has the potential to have synchronization errors. Thus the chip timing errors are defined as, $\tau_{11}, \tau_{12}, \ldots, \tau_{1L}$, and correspondingly, the carrier phase errors are defined as, $\phi_{11}, \phi_{12}, \ldots, \phi_{1L}$.

Following the same procedure outlined for the selection diversity receiver, one can write the error probability for maximal ratio combining conditioned on the L path gains and the

Gaussian random variable α as,

$$\begin{aligned} P(E|\beta_{11},\ldots,\beta_{1L},\alpha) &= \frac{1}{2}-\frac{2}{\pi}\sum_{\substack{m=1\\ m\text{ odd}}}^{\infty}\frac{1}{m}e^{-m^2\omega^2/2} \\ &\cdot\sin\left[\frac{m\omega\sqrt{2P_1}\sum_{j=1}^{L}\beta_{1j}^2\cos(\phi_{1j})[G(T_c-\tau_{1j})-\alpha\tau_{1j}]}{\sigma_N}\right] \\ &\Phi_I\left(-\frac{m\omega}{\sigma_N}\right)\Phi_M\left(-\frac{m\omega}{\sigma_N}\right). \end{aligned} \tag{75}$$

Once again, we only need to find the characteristic functions of I and M to find the error probability expression. These functions can be found either semi-analytically or using the independence assumption discussed in the previous section. Using the equations (9.1.18) on page 360 of [29] and (6.629) on page 716 of [28], we obtain,

$$\begin{aligned} \Phi_I(\omega) &= \left[\frac{1}{2}e^{-\omega^2P_1\rho_0T_c^2(\sum_{j=1}^{L}\beta_{1j})^2}+\frac{1}{2}\sum_{n=0}^{\infty}\frac{n!(\omega\sqrt{P_1\rho_0}T_c(\sum_{j=1}^{L}\beta_{1j}))^{2n}}{(2n+1)!}\right. \\ &\left.\cdot M(n+1,2(n+1),-\omega^2P_1\rho_0T_c^2(\sum_{j=1}^{L}\beta_{1j})^2)\right]^{G(L-1)}, \end{aligned} \tag{76}$$

and

$$\begin{aligned} \Phi_M(\omega) &= \left[\frac{1}{2}e^{-\omega^2P_k\rho_0T_c^2(\sum_{j=1}^{L}\beta_{1j})^2}+\frac{1}{2}\sum_{n=0}^{\infty}\frac{n!(\omega\sqrt{P_k\rho_0}T_c(\sum_{j=1}^{L}\beta_{1j}))^{2n}}{(2n+1)!}\right. \\ &\left.\cdot M(n+1,2(n+1),-\omega^2P_k\rho_0T_c^2(\sum_{j=1}^{L}\beta_{1j})^2)\right]^{GL(K-1)}. \end{aligned} \tag{77}$$

It is possible to uncondition (75) from the random varible α analytically. The error probability conditioned only on the individual path gains is given by,

$$\begin{aligned} &P(E|\beta_{11},\ldots,\beta_{1L}) \\ &= \frac{1}{2}-\frac{2}{\pi}\sum_{\substack{m=1\\ m\text{ odd}}}^{\infty}\frac{1}{m}e^{-m^2\omega^2/2}\exp(-m^2\omega^2P_1G(\sum_{j=1}^{L}\beta_{1j}^2\cos(\phi_{1j})\tau_{1j})^2/\sigma_N^2) \\ &\quad\cdot\sin\left[\frac{m\omega\sqrt{2P_1}\sum_{j=1}^{L}\beta_{1j}^2\cos(\phi_{1j})G(T_c-\tau_{1j})}{\sigma_N}\right]\Phi_I\left(-\frac{m\omega}{\sigma_N}\right)\Phi_M\left(-\frac{m\omega}{\sigma_N}\right) \end{aligned} \tag{78}$$

Unconditioning (78) from the individual path fains requires numerical integration. We use the simple trapezoidal rule to perform this integration.

IV.3 Equal Gain Combining

When equal gain combining is employed, the receiver simply sums each path term and uses this sum in the decision making. Then,

$$\begin{aligned} Z &= \sum_{j=1}^{L} Z_{1j} \\ &= \sum_{j=1}^{L} D_{1j} + I_{1j} + M_{1j} + N_{1j} \\ &= D + I + M + N \end{aligned} \tag{79}$$

where D is the sum of the desired signal terms from all branches, I is the intersymbol interference, M is the multiple access interference and N is the AWGN term with variance equal to,

$$\sigma_N^2 = N_0 T L. \tag{80}$$

Similar to the maximal ratio combining case, when equal gain combining is employed, it is clear from (79) that all of the L paths are used in the decision making process. Therefore, the chip timing errors are defined as, $\tau_{11}, \tau_{12}, \ldots, \tau_{1L}$ and similarly, the carrier phase errors are defined as, $\phi_{11}, \phi_{12}, \ldots, \phi_{1L}$.

Following the same procedure outlined for the selection diversity receiver one can write the error probability for equal gain combining conditioned on the L path gains and α as,

$$\begin{aligned} P(E|\beta_{11}, \ldots, \beta_{1L}, \alpha) &= \frac{1}{2} - \frac{2}{\pi} \sum_{\substack{m=1 \\ m \text{ odd}}}^{\infty} \frac{1}{m} e^{-m^2\omega^2/2} \\ &\cdot \sin\left[\frac{m\omega\sqrt{2P_1}\sum_{j=1}^{L} \beta_{1j}\cos(\phi_{1j})[G(T_c - \tau_{1j}) - \alpha\tau_{1j}]}{\sigma_N}\right] \\ &\cdot \Phi_I\left(-\frac{m\omega}{\sigma_N}\right) \cdot \Phi_M\left(-\frac{m\omega}{\sigma_N}\right). \end{aligned} \tag{81}$$

The characteristic functions are found the same way as in the two previous cases as,

$$\begin{aligned} \Phi_I(\omega) &= [\frac{1}{2} e^{-\omega^2 P_1 \rho_0 T_c^2} + \frac{1}{2} \sum_{n=0}^{\infty} \frac{n!(\omega\sqrt{P_1\rho_0}T_c)^{2n}}{(2n+1)!} \\ &\cdot M(n+1, 2(n+1), -\omega^2 P_1 \rho_0 T_c^2)]^{G(L-1)}, \end{aligned} \tag{82}$$

and

$$\begin{aligned} \Phi_M(\omega) &= [\frac{1}{2} e^{-\omega^2 P_k \rho_0 T_c^2} + \frac{1}{2} \sum_{n=0}^{\infty} \frac{n!(\omega\sqrt{P_k\rho_0}T_c)^{2n}}{(2n+1)!} \\ &\cdot M(n+1, 2(n+1), -\omega^2 P_k \rho_0 T_c^2)]^{GL(K-1)}. \end{aligned} \tag{83}$$

Similar to the maximal ratio case, it is possible to uncondition the error probability expression from the variable α analytically,

$$\begin{aligned} P(E|\beta_{1j}) &= \frac{1}{2} - \frac{2}{\pi} \sum_{\substack{m=1 \\ m \text{ odd}}}^{\infty} \frac{1}{m} e^{-m^2\omega^2/2} \exp(-m^2\omega^2 P_1 G (\sum_{j=1}^{L} \beta_{1j}\cos(\phi_{1j})\tau_{1j})^2/\sigma_N^2) \\ &\cdot \sin\left[\frac{m\omega\sqrt{2P_1}\sum_{j=1}^{L}\beta_{1j}\cos(\phi_{1j})G(T_c-\tau_{1j})}{\sigma_N}\right] \Phi_I\left(-\frac{m\omega}{\sigma_N}\right)\Phi_M\left(-\frac{m\omega}{\sigma_N}\right) \end{aligned} \quad (84)$$

However, as before, unconditioning (75) from the individual path gain variables requires numerical integration. Once again, we use the trapezoidal rule for this purpose.

IV.4 Computational Aspects

The error probability expressions for the three diversity combining schemes, (70), (78) and (84) can be proved to be absolutely convergent [30]. Note once again that ω is the Fourier series frequency. Thus the above expressions for the probability of error are strictly true in the limit as ω goes to zero. In our case, we find that it is sufficient to assume $\omega = \pi/25$ and correctly calculate error probabilities greater than or equal to 10^{-7} with negligible error. The accuracy of the technique is clearly bounded by the truncation of the infinite series. In our case, taking the first 21 terms in the series into consideration was sufficient to achieve the desired level of accuracy. Bounds on the truncation error have been discussed in detail in [22].

V Degradation of the System Capacity due to Synchronization Errors

For the three different receiver structures considered in this paper the probability of error, as can be observed in 70), (78) and (84), is a function of the received signal to noise ratio, SNR=$2\rho_0 P_1 T/N_0$, the number of users present in the system, K, the number of diversity paths, L, the synchronization errors, τ_{1j} and ϕ_{1j} and the processing gain, G. Thus, it is possible to find the system capacity for different values of SNR, number of diversity paths, synchronization errors and processing gain. When G, SNR, L, τ_{1j} and ϕ_{1j} are fixed, we can evaluate the error probability of the system for increasing number of users. The capacity of the system is simply the maximum number of users that will still yield an error probability below a certain threshold.

We consider a voice transmission at 9600 bits/sec that requires an error probability $\leq 10^{-3}$ and system bandwidths of 1.25 MHz, 5MHz and 10MHz. The 1.25MHz system has a processing gain of 128, the 5MHz system has a processing gain of 512 and the 10MHz system has a processing gain of 1024. We assume that the maximum multipath delay spread is in the range of 25 to 200 nanoseconds [31]. Thus, we conclude that the 1.25MHz channel has only one, the 5MHz channel has two and the 10MHz system has three resolvable paths. We assume a slowly fading channel.

For all three diversity combining schemes, multipath fading affects the system performance dramatically. The 1.25MHz system at 20dB SNR has a capacity of zero if no coding and diversity is employed and no voice activity factor is taken into account. The same system was shown to have a capacity of 39 users in an AWGN environment [9, 19]. As stated previously, the 1.25MHz system has no inherent diversity through multipath; other means such as the use of multiple antennas at the receiver are to be employed to achieve a nonzero capacity. When an artificial diversity of 2 is achieved, the system has a capacity of 4 if selection diversity is employed, 9 if equal gain combining is employed and 13 if maximal ratio combining is employed.

The wideband systems of 5MHz and 10MHz, on the other hand, both have resolvable multipath branches of 2 and 3, respectively. If all of these branches are utilized by means of selection diversity at the receiver, the 5MHz system has a capacity of 17 and the 10MHz system has a capacity of 58, respectively.

Synchronization errors effect the system capacity significantly. For example, for the 1.25MHz system with 2 artificial multipaths, a chip timing error of 10% will reduce capacity of the selection diversity system to 3, the capacity of the equal gain combining system to 7 and the capacity of the maximal ratio combining system to 10, a 20% reduction in the system capacity in all cases. This percentage loss in the system capacity is approximately the same as the percentage loss of the same system in the AWGN environment [19]. Here, we assume that for maximal ratio and equal combining systems, all of the receiver branches suffer from the same level of synchronization errors, i.e., $\tau_{11} = \tau_{12} = \ldots = \tau_{1L}$ and $\phi_{11} = \phi_{12} = \ldots = \phi_{1L}$. From 70), (78) and (84), it can be seen that the synchronization errors effect the system performance by potentially reducing the energy of the desired signal component of the received signal and by introducing self interference. We have numerically found that the self interference, in comparison to the signal energy reduction is negligibly small. The reduction in the desired signal energy level can alternatively be interpreted as an effective processing gain loss. Then, the effective processing gain is approximately a linear function of the system capacity for a given level of maximum allowable error probability.

System error probabilities as a function of SNR are plotted for the three diversity combining schemes when perfect synchronization is achieved in Figure 5. For the selection diversity receiver, the capacity losses for various levels of synchronization errors are listed in tabular form in Table 1 for the 1.25MHz system, in Table 2 for the 5MHz system and in Table 3 for the 10MHz system, respectively, all at 20dB SNR. From these tables, it can be seen that the percentage capacity loss due to a certain level of synchronization error is approximately the same in all three systems independent of the number of diversity branches considered. The occasional discrepencies between the values are due to the quantization inherent in the process of finding the system capacity from the bit error rate. This is because, the system capacity can only take on integer values.

In Tables 4 and 5, the capacity losses of the three diversity combining schemes are compared for various chip timing and carrier phase error values when the system bandwitdh is 1.25MHz and 5MHz, respectively. It is seen that the percentage capacity losses due to a certain level of synchronization error are approximately the same for the three diversity schemes. Thus, it can be concluded that all three diversity combining schemes are equally sensitive to synchronization errors.

In a practical system, both chip timing and carrier phase errors will be present. If we define the capacity loss of a system as the difference between the capacity when there are no synchronization errors and the capacity when synchronization errors are present, it can be seen from Tables 1-5 that the capacity loss from the presence of both chip timing and carrier phase errors is approximately the sum of individual losses for all values of SNR for all systems considered.

Error probability as a function of the number of active users present in the system is plotted in Figures 6, 7 and 8 for the 1.25MHz, 5MHz and 10MHz systems, respectively when selection diversity is employed. The graphs show that as the number of users increase, the performance of systems with different number of diversity paths converge. However, when low error probabilities are required, as is the case for reliable transmission of voice, data and video signals, having multiple diversity branches increase the system performance that was reduced by fading. However, diversity combining on its own, is not sufficient to gain back all of the capacity that is lost due to fading. Additional means such as coding, interleaving and/or antenna diversity are necessary to further increase the capacity. It is seen from Figures 7 and 8 that when the multipath branches inherent in the 5MHz and 10MHz systems are not utilized (i.e. when L=1 for the 5MHz system and when L=1,2 for the 10MHz system), the performance of these systems become almost as poor as the 1.25MHz system that does not employ any diversity.

VI Conclusions

An infinite series for the probability of error of a BPSK modulated DS CDMA system with nonzero chip timing and carrier phase errors in a slowly fading, multipath environment can be derived using the Fourier series approach of [22] when the coherent RAKE receiver employs selection diversity, equal gain combining or maximal ratio combining. The expression does not resort to the widely used Gaussian approximation. Computation of error probabilities using the series is fast. In fact, it takes approximately 3-4 minutes to generate data for a whole bit error rate curve of ten points using a Sparc 20 work station.

For all diversity schemes considered, a capacity drop due to the presence of different types of synchronization errors is found to be approximately equal to the sum of the capacity losses due to the presence of each of these synchronization errors alone. The reduction in the system capacity is found to be mainly due to the reduction in the energy level of the desired signal component of the received signal. Thus, this reduction can be interpreted as a potential loss in the processing gain.

It is also concluded that fading reduces the system capacity dramatically. The 1.25MHz system which has a capacity of 39 users in an AWGN environment, has 0 capacity when the environment is slowly fading. The system capacity can be increased by introducing diversity. Among the three diversity schemes, as expected, maximal ratio combining grants the highest capacity increase. The synchronization errors cause a further reduction on the system capacity. We found that, similar to the AWGN channel case, for the typical case of a DS CDMA system with an SNR of 20dB, a 10% timing error causes approximately a 20% capacity loss regardless of the processing gain of the system. Therefore, accurate chip synchronizers are needed in a practical system that employs DS CDMA. The reduction in the capacity due to synchronization errors appears to be approximately the same regardless of the channel; AWGN channels are equally effected by the synchronization errors as the slowly fading, multipath channels that use one of the three diversity combining schemes considered.

When the system bandwidth is increased to 5MHz or 10MHz, the system enjoys inherent diversity. A receiver that makes use of these branches by using a diversity combining technique achieves a much higher capacity than the 1.25MHz system. However, if the multipath branches are not utilized, the system performance goes down almost to the level of the performance of the 1.25MHz system.

References

[1] K.S. Gilhousen, I.M. Jacobs, R. Padovani and L.A. Weaver, Jr., "Increased Capacity Using CDMA For Mobile Satellite Communication," *IEEE Journal on Selected Areas in Communications*, vol. 8, no. 4, pp. 503-514, May 1990.

[2] K.S. Gilhousen, I.M. Jacobs, R. Padovani, A.J. Viterbi, L.A. Weaver, Jr. and C.E. Wheatley III, "On the Capacity of a Cellular CDMA System," *IEEE Transactions on Vehicular Technology*, vol. 40, no. 2, pp. 303-312, May 1991.

[3] A.J. Viterbi, *CDMA: Principles of Spread Spectrum Communication.* Reading: Addison-Wesley, 1995.

[4] M.O. Sunay, "IS-95 Evolution Towards the Third Generation System," *Proceedings of the IEEE Sarnoff Symposium on Advances in Wired and Wireless Communications,* Trenton, pp. 115-119, March 18, 1998.

[5] J.G. Proakis, *Digital Communications*, 2nd ed., New York: McGraw-Hill, 1989.

[6] D.G. Brennan, "Linear Diversity Combining Techniques," *Proceedings of the IRE*, vol. 47, pp. 1075-1102, June 1959.

[7] J.M. Holtzman, "A Simple, Accurate Method to Calculate Spread Spectrum Multiple Access Error Probabilities," *IEEE Transactions on Communications*, vol. 40, no. 3, pp. 461-464, March 1992.

[8] D.J. Torrieri, "Performance of Direct-Sequence Systems with Long Pseudonoise Sequences," *IEEE Journal on Selected Areas in Communications*,vol. 10, no. 4, pp. 770-781, May 1992.

[9] F. Bartucca and E. Biglieri, "DS SSMA Capacity for a Mobile Satellite System," *Proceedings of IMSC'93 Conference*, pp. 461-466, June 16-18 1993.

[10] E.S. Sousa, "Performance of a Direct Sequence Spread Spectrum Multiple Access System Utilizing Unequal Carrier Frequencies," *IEICE Transactions on Communications*, vol. E76-k, no. 8, pp. 906-912, August 1993.

[11] F. Simpson and J. Holtzman, "On Calculating Bit Error Probability for Convolutional Coding Over the Ricean Fading Channel", *Proceedings of IEEE VTC'92 Conference*, pp.271-274, 1992

[12] R. Prasad, A. Kegek and O.L. van Linden, "Performance Evaluation of Microcellular Systems with Shadowed Ricean/Rayleigh Faded Multiple Co-Channel Interferers," *Proceedings of IEEE VTC'92 Conference*, pp. 427-430, 1992.

[13] L.B. Milstein, T.S. Rappaport and R. Barghoutti, "Performance Evaluation for Cellular CDMA," *IEEE Journal on Selected Areas in Communicaitons*, vol. 10, no. 4. pp. 680-689, May 1992.

[14] G.L. Stüber, "Analysis of a Multiple-Cell Direct-Sequence CDMA Cellular Mobile Radio System," *IEEE Journal on Selected Areas in Communications*, vol. 10, no. 4, pp. 669-679, May 1992.

[15] S. Souissi and S.B. Wicker, "A Diversity Combining DS CDMA System with Convolutional Encoding and Viterbi Decoding," *IEEE Transactions on Vehicular Technology,* vol. 44, no. 2, pp. 304-312, May 1995.

[16] M.O. Sunay and P.J. McLane, "Calculating Error Probabilities for DS CDMA Systems: When Not to Use the Gaussian Approximation," *Proceedings of the IEEE GLOBERCOM'96 Conference,* London, UK, pp. 1744-1749, November 18-22, 1996.

[17] M.O. Sunay and P.J. McLane, " Diversity Combining for DS CDMA Systems," *Proceedings of the IEEE ICC'96 Conference,* Dallas, Texas, pp. 83-89, June 23-27, 1996.

[18] M.O. Sunay and P.J. McLane, " Effects of Carrier Phase and Chip Timing Errors on the Capacity of a Quadriphase Spread BPSK Modulated DS CDMA System," *Proceedings of IEEE GLOBECOM'95 Conference*, Singapore, pp. 1114-1120, November 13-17 1995.

[19] M.O. Sunay and P.J. McLane, "Sensitivity of a DS CDMA System with Long PN Sequences to Synchronization Errors," *Proceedings of IEEE ICC'95 Conference*, Seattle, pp. 1029-1035, June 18-22 1995.

[20] M. Kavehrad and P.J. McLane, "Performance of Low-Complexity Channel Coding and Diversity for Spread Spectrum in Indoor, Wireless Communication," *Bell System Technical Journal*, vol. 64, no. 8, pp. 1927-1965, October 1985.

[21] J. Panicker, S. Kumar, "Effect of System Imperfections on BER Performance of CDMA Correlator Receiver," *Proceedings of the IEEE ICC'95 Conference,* Seattle, pp. 894-899, June 18-22, 1995.

[22] N.C. Beaulieu, "The Evaluation of Error Probabilities for Intersymbol and Cochannel Interference," *IEEE Transactions on Communications*, vol. 39, no. 12, pp. 1740-1749, December 1991.

[23] W.C. Jakes, ed., *Microwave Mobile Communications*, reissue, New York: IEEE Press, 1994.

[24] G.L. Turin, "On Optimal Diversity Reception," *IRE Transactions on Information Theory,* vol. IT-7, pp. 22-31, July 1961.

[25] Y.C. Yoon, R. Kohno and H. Imai, "A Spread Spectrum Multiaccess System with Cochannel Interference Cancellation for Multipath Fading Channels," *IEEE Journal on Selected Areas in Communications,* vol. 11, no. 7, pp. 1067-1075, September 1993.

[26] M.B. Pursley, "Performance Evaluation for Phase-Coded Spread Spectrum Multiple Access Communication - Part I: System Analysis," *IEEE Transactions on Communications,* vol. COM-25, pp. 795-799, August 1977.

[27] A. Papoulis, *Probability, Random Variables, and Stochastic Processes*, 3rd ed., New York: McGraw-Hill, 1991.

[28] I.S. Gradshteyn and I.M. Ryzhik, *Table of Integrals, Series and Products.* San Diego: Academic Press, 1980.

[29] M. Abramowitz and I.A. Stegun, *Handbook of Mathematical Functions.* New York: Dover Publications, 1972.

[30] M.O. Sunay, *Performance Analysis of Direct Sequence Code Division Multiple Access Systems.* Ph.D. Dissertation, Queen's University at Kingston, 1998.

[31] A. Jalali and P. Mermelstein, "Effects of Diversity, Power Control and Bandwidth on the Capacity of Microcellular CDMA Systems," *IEEE Journal on Selected Areas in Communications* , vol. 12, pp. 952-961, June 1994.

G=128 (BW=1.25MHz), P(E)=10^{-3}, SNR=20dB		
Synchronization Errors	Capacity	Percentage Capacity Loss wrt Perfect Synchronization Case
L=1		
perf. synch.	0	
L=2		
perf. synch.	4	
$T_c/10$	3	25%
$T_c/25$	4	0%
$T_c/50$	4	0%
$\pi/5$	3	25%
$\pi/10$	4	0%
$\pi/20$	4	0%
$T_c/10, \pi/10$	3	25%
L=3		
perf. synch.	7	
$T_c/10$	6	14.29%
$T_c/25$	6	14.29%
$T_c/50$	7	0%
$\pi/5$	4	42.86%
$\pi/10$	6	14.29%
$\pi/20$	7	0%
$T_c/10, \pi/10$	5	28.57%
L=5		
perf. synch.	9	
$T_c/10$	7	22.22%
$T_c/25$	8	11.11%
$T_c/50$	8	11.11%
$\pi/5$	5	44.44%
$\pi/10$	8	11.11%
$\pi/20$	8	11.11%
$T_c/10, \pi/10$	6	33.33%

Table 1: Capacity losses due to different levels of synchronization errors for the 1.25MHz system at 20dB when selection diversity is employed.

G=512 (BW=5MHz), P(E)=10^{-3}, SNR=20dB		
Synchronization Errors	Capacity	Percentage Capacity Loss wrt Perfect Synchronization Case
L=2		
perf. synch.	17	
$T_c/10$	13	23.53%
$T_c/25$	16	5.88%
$T_c/50$	17	0%
$\pi/5$	10	41.18%
$\pi/10$	15	11.76%
$\pi/20$	17	0%
$T_c/10, \pi/10$	12	29.41%
L=4		
perf. synch.	33	
$T_c/10$	27	18.18%
$T_c/25$	30	9.09%
$T_c/50$	32	3.03%
$\pi/5$	21	36.36%
$\pi/10$	30	9.09%
$\pi/20$	32	3.03%
$T_c/10, \pi/10$	24	27.27%
L=6		
perf. synch.	34	
$T_c/10$	27	20.59%
$T_c/25$	31	8.82%
$T_c/50$	33	2.94%
$\pi/5$	22	35.29%
$\pi/10$	31	8.82%
$\pi/20$	33	2.94%
$T_c/10, \pi/10$	25	26.47%

Table 2: Capacity losses due to different levels of synchronization errors for the 5MHz system at 20dB when selection diversity is employed.

G=1024 (BW=10MHz), P(E)=10^{-3}, SNR=20dB		
Synchronization Errors	Capacity	Percentage Capacity Loss wrt Perfect Synchronization Case
L=3		
perf. synch.	58	
$T_c/10$	46	20.69%
$T_c/25$	53	8.62%
$T_c/50$	56	3.45%
$\pi/5$	36	37.93%
$\pi/10$	52	10.34%
$\pi/20$	57	1.72%
$T_c/10, \pi/10$	41	29.31%
L=6		
perf. synch.	69	
$T_c/10$	55	20.29%
$T_c/25$	63	8.69%
$T_c/50$	66	4.35%
$\pi/5$	44	36.23%
$\pi/10$	62	10.14%
$\pi/20$	67	2.89%
$T_c/10, \pi/10$	49	28.99%

Table 3: Capacity losses due to different levels of synchronization errors for the 10MHz system at 20dB when selection diversity is employed.

G=128 (BW=1.25MHz), P(E)=10^{-3}, SNR=20dB, L=2			
	System Capacity		
Synchronization Errors	Selection Diversity	Equal Gain Combining	Maximal Ratio Combining
perf. synch.	4	9	13
$T_c/10$	3	7	10
$T_c/25$	4	8	12
$\pi/5$	3	5	7
$\pi/10$	4	8	11
$T_c/10, \pi/10$	3	6	9

Table 4: Capacity losses due to different levels of synchronization errors for the 1.25 system at 20dB when selection diversity, equal gain combining and maximal ratio combining is employed.

G=512 (BW=5MHz), P(E)=10^{-3}, SNR=20dB, L=2			
	System Capacity		
Synchronization Errors	Selection Diversity	Equal Gain Combining	Maximal Ratio Combining
perf. synch.	17	35	50
$T_c/10$	13	28	39
$T_c/25$	16	32	46
$\pi/5$	10	21	28
$\pi/10$	15	33	43
$T_c/10, \pi/10$	12	24	35

Table 5: Capacity losses due to different levels of synchronization errors for the 5MHz system at 20dB when selection diversity, equal gain combining and maximal ratio combining is employed.

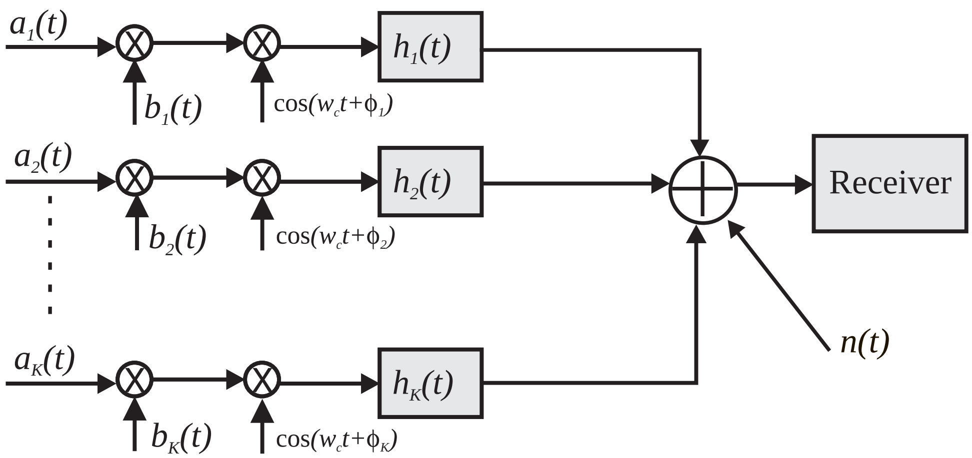

Figure 1: DS CDMA System Model

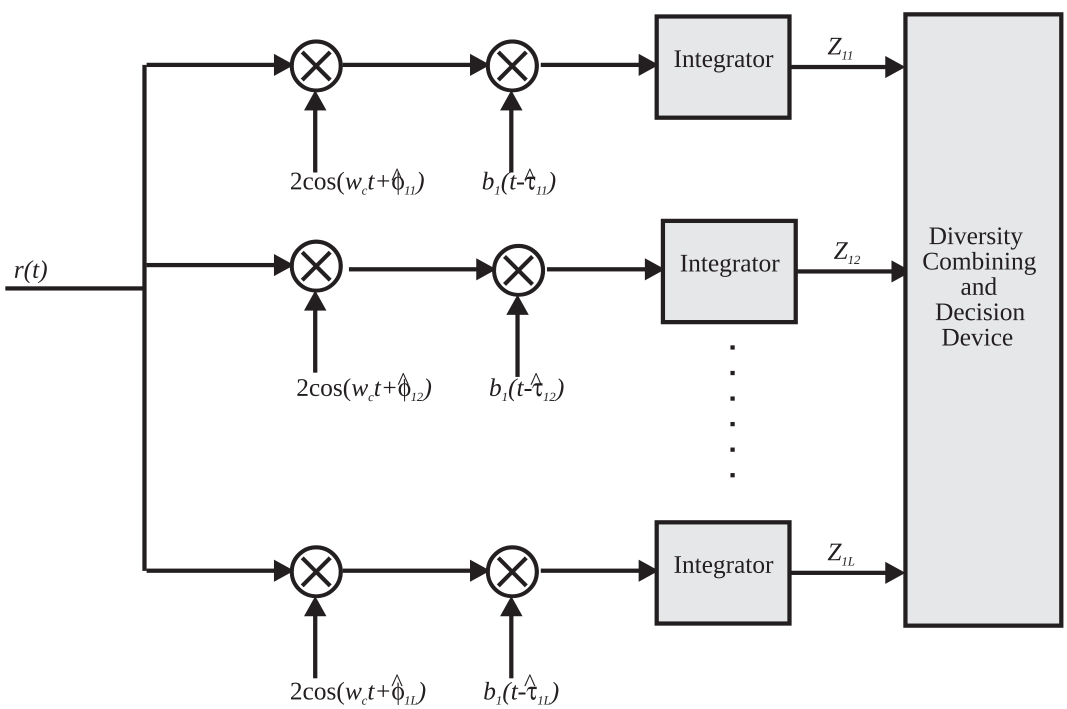

Figure 2: L-Branch Coherent RAKE Receiver for the Multipath Fading Channel

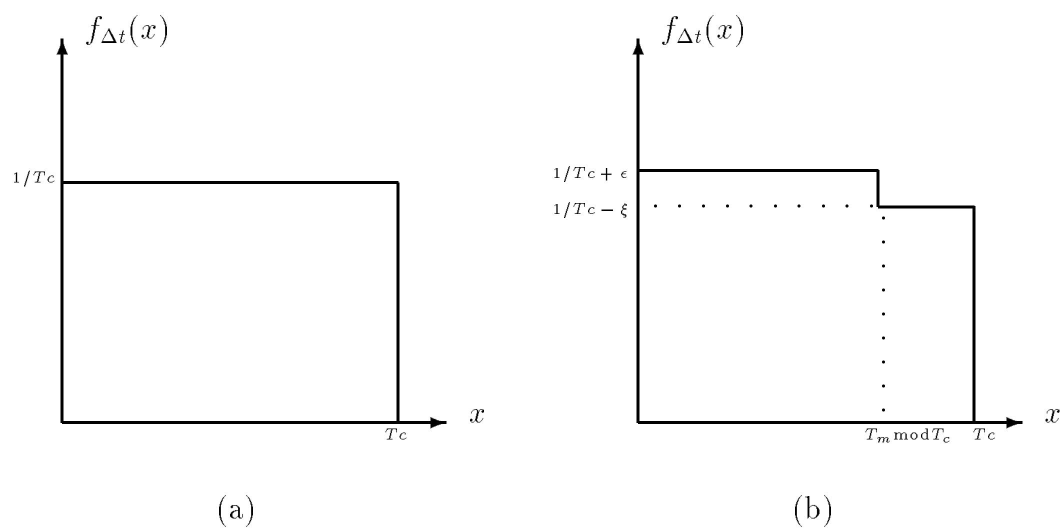

Figure 3: The probability density function of Δt_{1l} when (a) T_m is an integer multiple of T_c (b) T_m is not an integer multiple of T_c

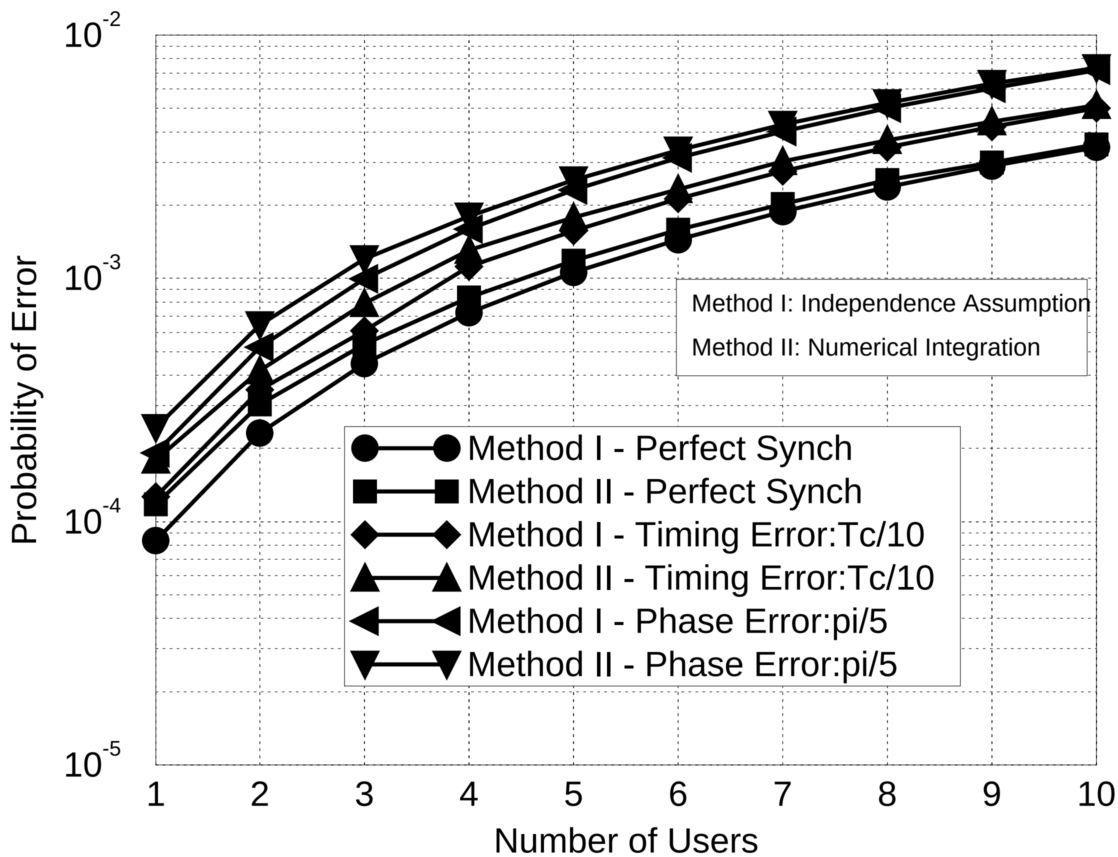

Figure 4: Comparison of the two methods in evaluating the system capacity for a system employing selection diversity on 2 paths and operating at 20dB SNR.

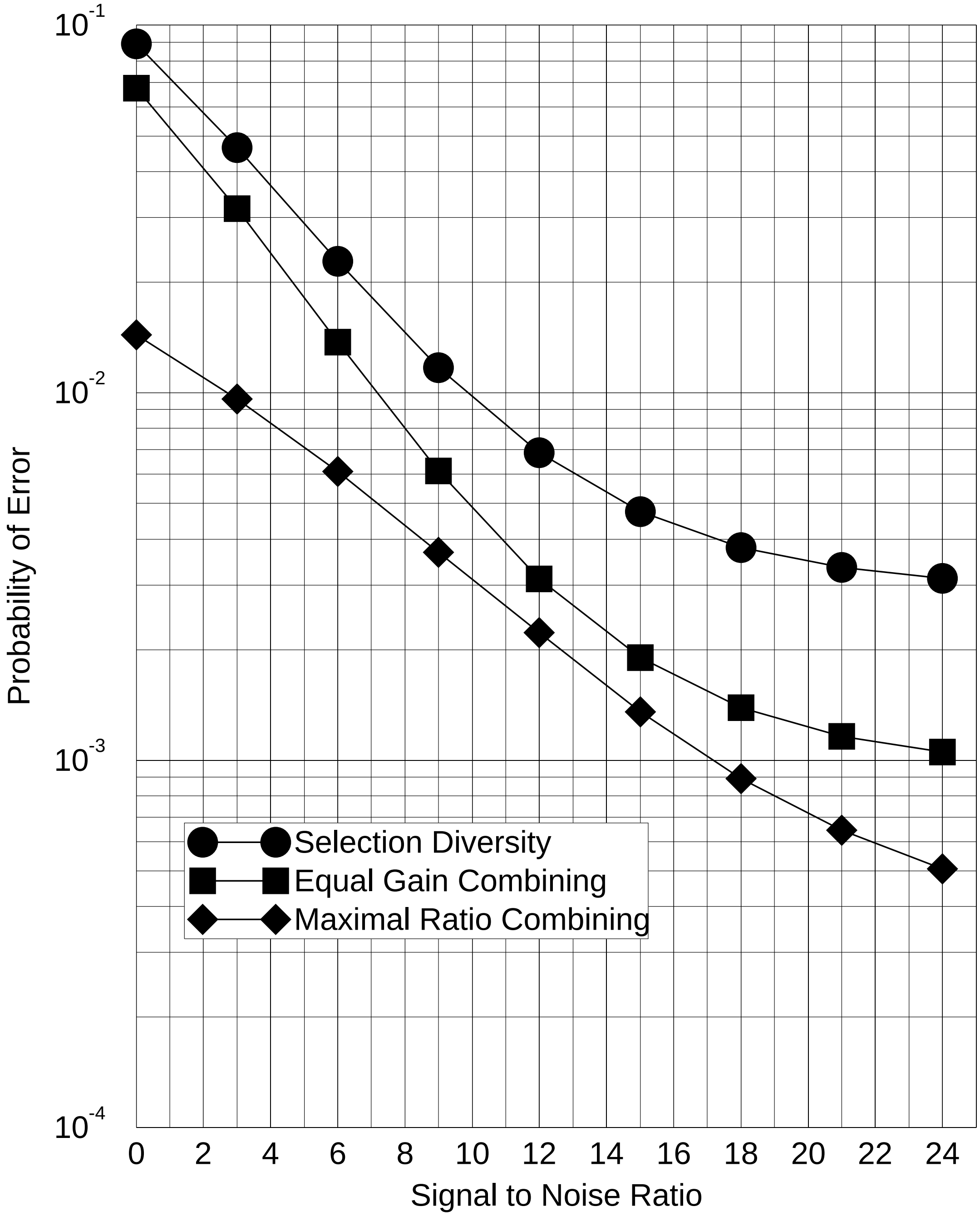

Figure 5: Comparison of the diversity combining schemes for the 1.25MHz system at 20dB when there are no synchronization errors.

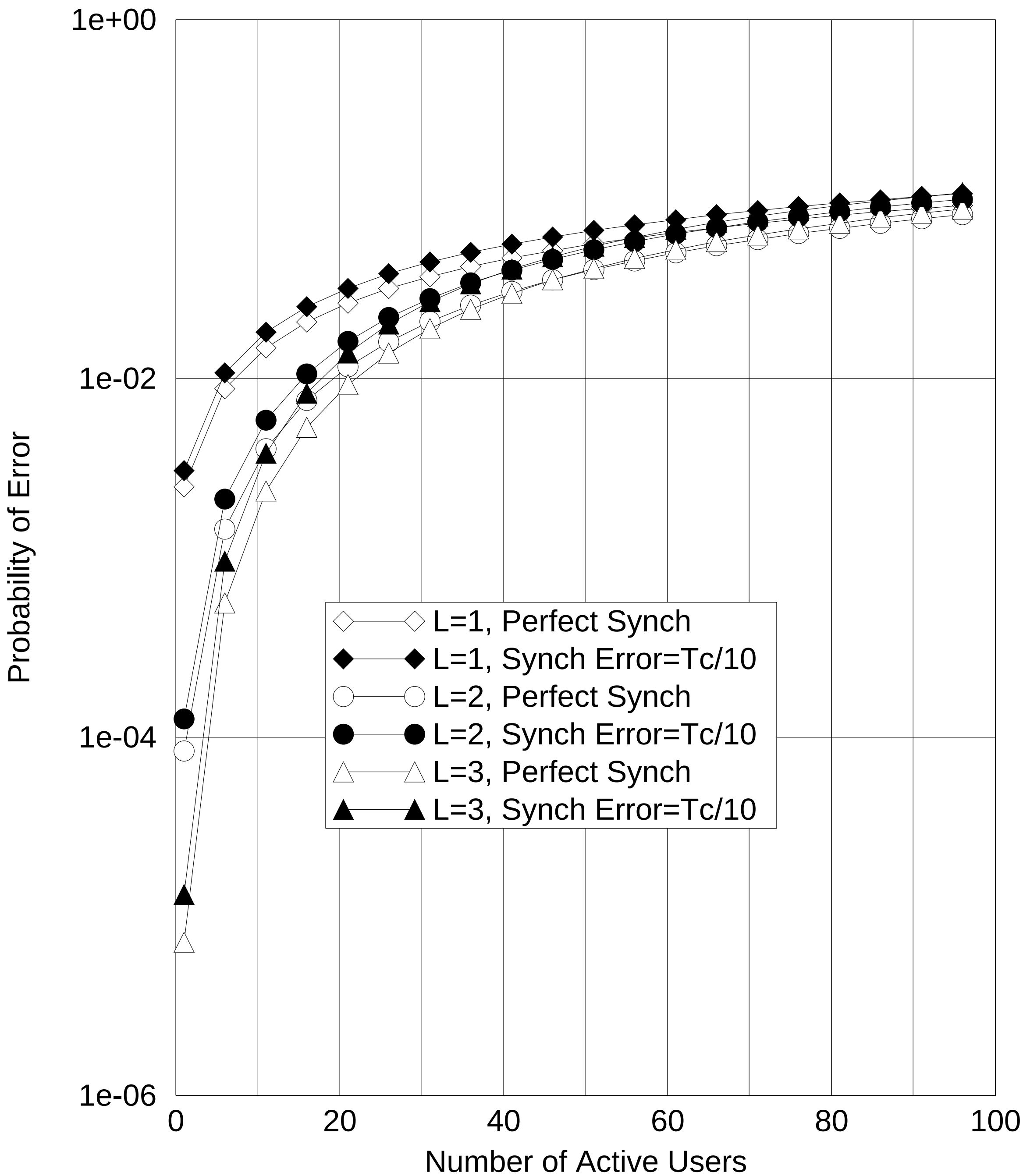

Figure 6: Probability of error versus the number of active users for the 1.25MHz system using various number of diversity branches when there are no synchronization errors and when there is a timing error of $T_c/10$ (Selection Diversity).

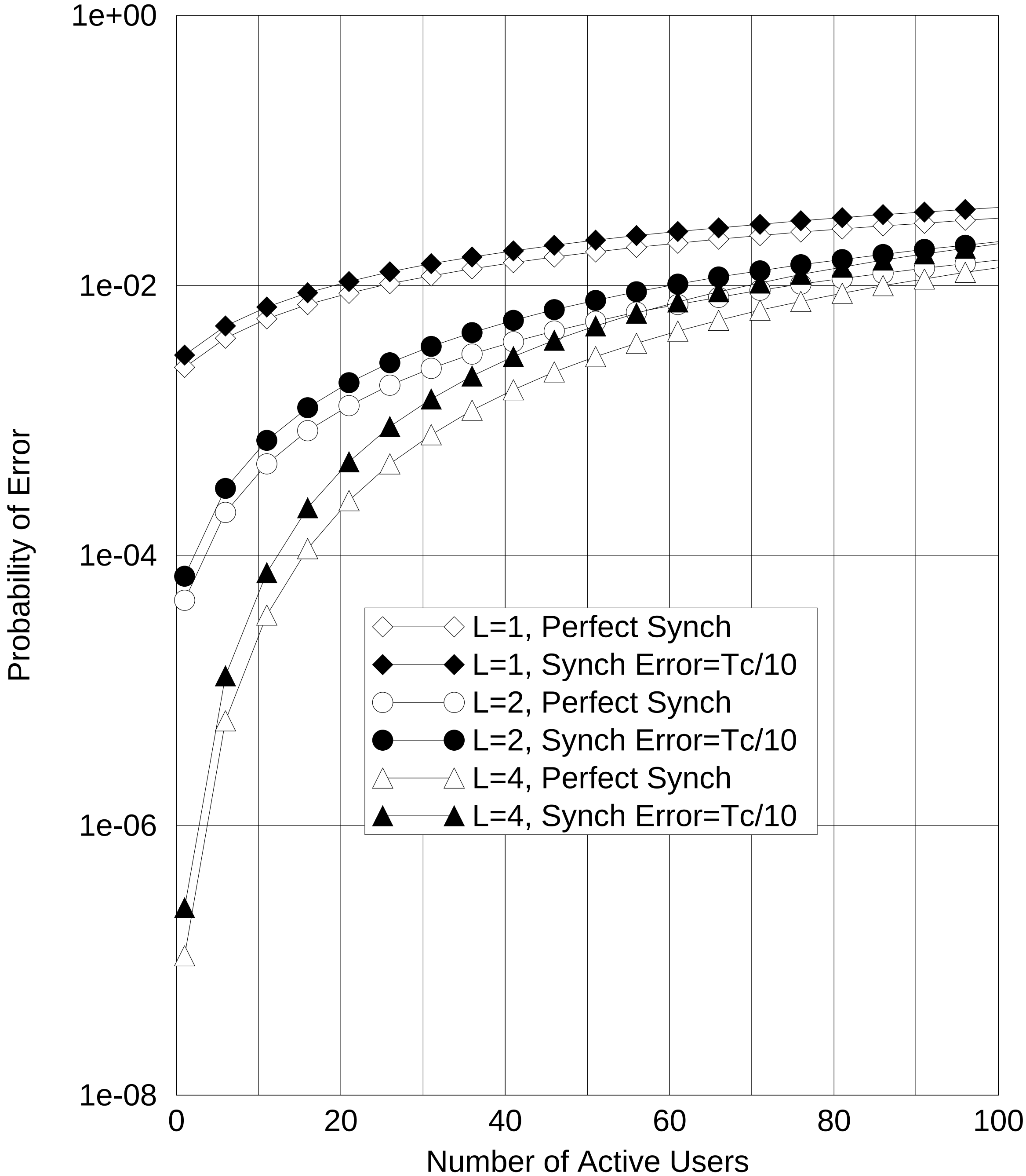

Figure 7: Probability of error versus the number of active users for the 5MHz system using various number of diversity branches when there are no synchronization errors and when there is a timing error of $T_c/10$ (Selection Diversity).

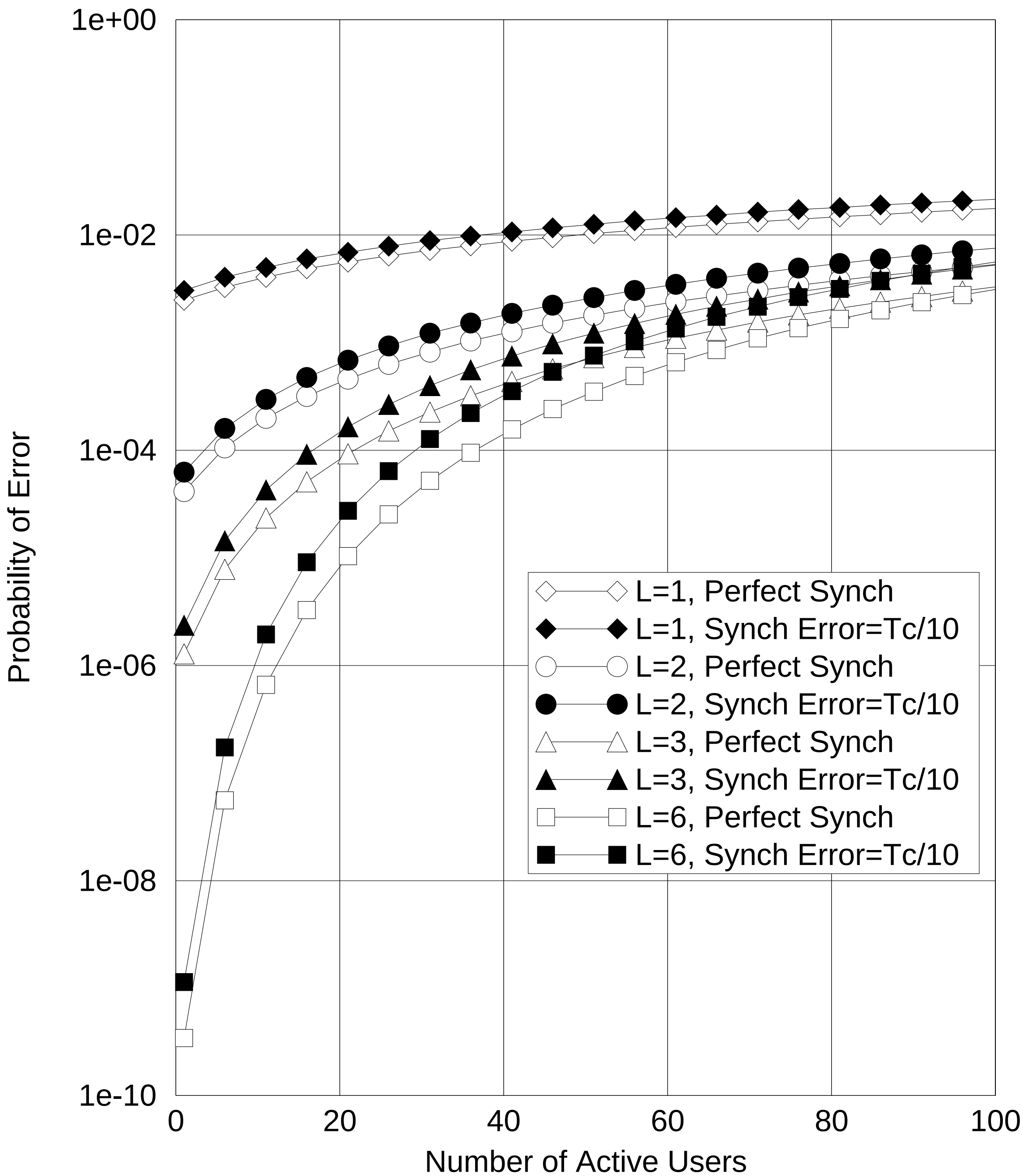

Figure 8: Probability of error versus the number of active users for the 10MHz system using various number of diversity branches when there are no synchronization errors and when there is a timing error of $T_c/10$ (Selection Diversity).